Presented at the ICANS-21 Conference, 5-9 September 2005, Lisbon, Portugal

Large area deposition of microcrystalline silicon by microwave PECVD

J. Löffler[A], H.-J. Muffler[A], C. Devilee[A], A. Gajovic[B], P. Dubcek[B], D. Gracin[B], W.J. Soppe[A]

[A] ECN-Solar Energy, P.O. Box 1, 1755 ZG Petten, The Netherlands, T: +31 224 564421, F: +31 224 568214, E: loffler@ecn.nl
[B] Rudjer Boskovic Institute, 1000 Zagreb, Bijenicka 54, Croatia

corresponding author: J. Löffler, ECN-Solar Energy, P.O. Box 1, 1755 ZG Petten, The Netherlands,
T: +31 224 564421, F: +31 224 568214, E: loffler@ecn.nl

Abstract

Intrinsic microcrystalline and amorphous silicon layers have been deposited by Microwave PECVD on glass substrates under variation of the silane to hydrogen ratio. A series of samples deposited at higher total pressure and with lower microwave power than previously applied is presented. The plasma was studied by means of optical emission spectroscopy. With increasing silane fraction, the silane utilization as well as the H_α/SiH^* ratio in the plasma decrease, and the layers become more amorphous. The hydrogen content in the film and the refractive index of the material at 0.5 eV, an indicator for the density of the films, increase with increasing silane fraction. The higher total pressure and lower microwave power during deposition resulted in a strong improvement in the structural and opto-electrical properties of microcrystalline and amorphous silicon layers. The best amorphous layers have σ_{dark} of $6*10^{-10}$ S/cm, $\sigma_{ph}/\sigma_{dark}$ of $6*10^4$, R* below 0.1, and an Urbach tail Energy of 55 meV. For the microcrystalline layers close to the µc-Si/a-Si transition, σ_{dark} of $1*10^{-6}$ S/cm, $\sigma_{ph}/\sigma_{dark}$ of 16, and an Urbach tail Energy of 107 meV have been achieved.

PACS: 52.70.Kz, 52.77.Dq, 61.43.Dq, 84.60.Jt
Keywords: Microwave PECVD, microcrystalline silicon, amorphous silicon, FTIR, FTPS

1. Introduction

Thin-film crystalline silicon solar cells deposited at low temperature have a great potential for the realization of low-cost / high-efficiency solar cells. So called 'micromorph' silicon solar cells [1], consisting of a tandem structure of amorphous and microcrystalline silicon, have shown high efficiencies up to 14.7 % on a laboratory scale [2]. Due to the relatively large thickness of the microcrystalline absorber layer around 1-2 µm, a high deposition rate for this layer with uniform layer properties on large area is essential for cost effective mass production. Best solar cell results have been obtained so far by VHF PECVD [3, 4] and RF PECVD [2, 5] in the high power, high pressure depletion regime. Alternative deposition methods that are investigated are e.g. Hot-Wire CVD [6] and Expanding Thermal Plasma CVD [7].

We present here results on intrinsic microcrystalline silicon layers deposited by microwave PECVD making use of a linear plasma source in combination with a moving substrate, which allows very high uniformity both, in direction of the source, and in direction of the substrate transport. This technique has been developed and successfully transferred to industry for large-area and high-rate deposition of silicon nitride layers applied for anti-reflection, surface and bulk passivation of crystalline silicon solar cells [8].

Research on the application of this microwave technique for the deposition of microcrystalline silicon has started recently, demonstrating the potential of high deposition rates [9]. While the first layers suffered from severe post-deposition oxidation due to porosity, the adjustment of the deposition set-up [10] and subsequent parameter variation [11] has lead to denser layers, which however still appeared less dense than state-of-the-art material deposited by RF and VHF PECVD.

Starting from our previously best materials prepared at a substrate temperature of 300°C, a higher total pressure and lower microwave power has been applied to find optimised conditions for the deposition of dense, device quality material. We present here a series of samples prepared with a variation of the silane to hydrogen ratio, while the other process parameters remained constant.

2. Experimental

Undoped amorphous and microcrystalline silicon films have been deposited simultaneously on crystalline silicon wafers and on aluminosilicate glass (Corning 1737) in a single chamber microwave (MW) PECVD reactor, in which a substrate holder with a substrate area

of 60x15 cm^2 moves underneath a linear microwave source [10]. A mixture of H_2 and Ar is injected in the vicinity of the microwave source, while silane (SiH_4) diluted in H_2 is injected closer to the substrate [10]. In the present study, the silane fraction, defined as SiH_4 flow divided by the total of SiH_4, H_2, and Ar flows ($\Phi_{SiH4}/(\Phi_{SiH4} + \Phi_{H2} + \Phi_{Ar})$), was varied between 1 % and 40 %. We aimed for a layer thickness of 1 µm.

Optical emission spectroscopy (OES) in the wavelength range from 200 to 1000 nm has been performed during deposition, and the characteristic lines for H_α and SiH^* in the plasma, at 656 nm and 412 nm, respectively, have been analysed.

From FTIR measurements between 400 cm^{-1} and 4000 cm^{-1}, performed with a Perkin Elmer BX II spectrometer, information on the hydrogen bonding as well as hydrogen concentration of the deposited films have been obtained. The microstructure factor R* has been determined as the fraction of the area of the Si-H_2 absorption peak at 2100 cm^{-1} and the sum of the areas of the peaks at 2000 cm^{-1} (Si-H) and 2100 cm^{-1}. The hydrogen content has been obtained from the integration of the absorption peak around 630 cm^{-1} [12], assuming a proportionality constant of 2.1×10^{19} cm^{-2}. The layer thickness and the refractive index at 0.5 eV have been obtained by fitting the interference fringes in the IR transmission spectra [10].

For the determination of the optical constants, the materials deposited on glass have been characterised by reflection and transmission measurements. A single-beam spectrophotometer equipped with an integrating sphere was applied, in order to exclude errors due to optical scattering of porous or rough layers. The absorption in the near-infrared has been determined by Fourier transform photocurrent spectroscopy (FTPS) [13].

The dark conductivity σ_d has been measured in 2-point configuration with a source-measure unit (Keithley) after applying Al electrodes on the layers. The photoconductivity σ_{ph} has been measured under simulated AM 1.5 light.

3. Results and Discussion

The inset of Fig. 1 shows the dependence of the intensity of the SiH* peak in the OES spectrum on the deposition rate obtained under variation of the silane concentration. For all figures in this paper the symbols depict measured points, while the lines are meant as guide to the eye. A linear correlation is found here between the deposition rate and SiH^* intensity, indicating that in the investigated process parameter regime, the intensity of the SiH^* peak is indeed a good representative of the concentration of the silicon species responsible for film growth. The growth rate of most of the layers varied between 0.05 and 0.15 nm/s. From Fig. 1 it can be seen that with increasing SiH_4 fraction in the source gas, the H_α/SiH^* ratio decreases rapidly in the regime where the fraction is below 5-10 %, and saturates at higher silane fractions. In the case of VHF PECVD, high values of H_α/SiH^* above 1 have been found to be an indicator for the transition from amorphous to microcrystalline films [14].

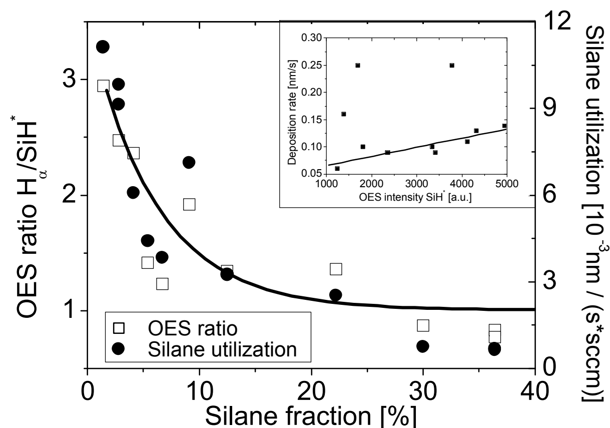

Figure 1. H_α/SiH^* ratio and silane utilization versus silane fraction in the source gas. The inset displays the linear relation between the deposition rate and the intensity of the SiH^* peak.

Interestingly, the silane utilization $\eta_{SiH4} = r_{dep}/\Phi_{SiH4}$, defined as the deposition rate divided by the silane flow, shows the same decreasing behavior at increasing SiH_4 fractions (see Fig. 1). This observation indicates that at higher silane fractions a lower depletion of SiH_4 is obtained. An explanation could be the fact that at higher silane flows the amount of remotely produced hydrogen and argon radicals is not sufficient to dissociate all the silane molecules injected at a position closer to the substrate.

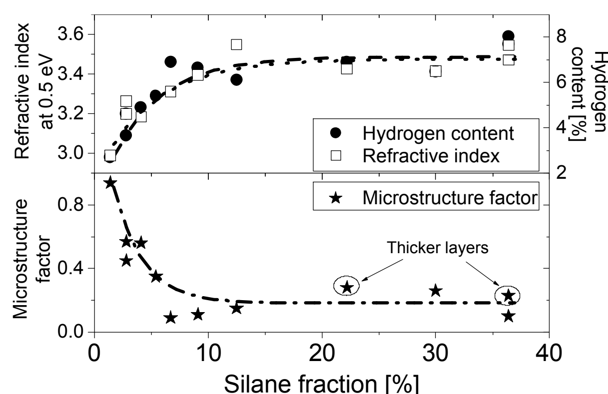

Figure 2. Refractive index at 0.5 eV, hydrogen content and microstructure factor as a function of the silane fraction.

Previous series of silicon layers deposited by microwave PECVD revealed relatively high porosity as reflected by low refractive indices and high post-oxidation rates [11].

This porosity appeared to be strongly correlated with the used silane fraction. In Figure 2, also a continuous decrease of the refractive index with decreasing silane fraction is demonstrated. But in this case, the mechanisms behind such a behavior are still to be resolved since the OES measurements give no indication of enhanced formation of sticky Si^* and SiH^* species at low (<5 %) silane fractions (i.e. low silane flows). The microstructure factor R*, as obtained from FTIR, can be correlated to the void density of amorphous Si layers. For device quality amorphous silicon, R* should be below 0.1 [15]. In microcrystalline layers, also hydrogen bonded to grain boundaries contributes to the 2100 cm^{-1} peak. In Fig. 2, R^* shows a steep drop from almost 1.0 to about 0.1 if the silane fraction is increased from 1 to 6 %. In this regime the material changes from microcrystalline to amorphous. For silane fractions >10 % the drop in microstructure factor is flattening. In this regime, apart from the silane flow during deposition, R^* is influenced by the layer thickness. Thicker layers (marked in Fig. 2) exhibit slightly higher R^* values, which might be due to a higher void density, or the nucleation of crystallites during growth. Note the increase in refractive index of $\Delta n = 0.2$ compared to our previous studies [11], and the low R^* values below 0.1 obtained for the amorphous layers deposited either close to the transition regime, or at very high silane fractions > 30 %.

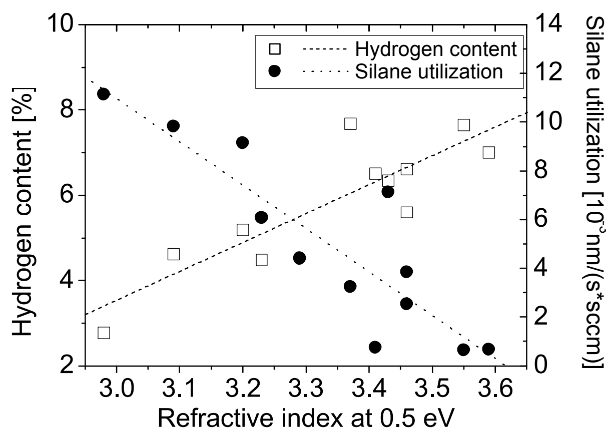

Figure 3. Hydrogen content and silane consumption as function of the refractive index at 0.5 eV.

The hydrogen content in the layers increases with increasing silane fraction, from about 3 % in the highly crystalline layers to about 8 % in the amorphous layers. These values are relatively low, which can be attributed to the relatively high substrate temperature of 300 °C. The lower hydrogen content and the higher R* for more crystalline layers indicate that the microcrystalline material is composed of crystallites with low hydrogen content in the bulk, and most of the hydrogen bonded at grain boundaries and voids, embedded in an amorphous matrix.

In Fig. 3, the hydrogen content and the silane utilization are plotted versus the refractive index at 0.5 eV, representing the density of the films. While the hydrogen content increases linearly with the refractive index, the silane utilization decreases almost linearly. Note that the decrease in silane utilization η_{SiH4} by a factor of 10 over the investigated regime of silane fractions is much larger than the possible increase of the density of the layers. This underlines our finding that compact amorphous silicon layers are grown under low silane depletion.

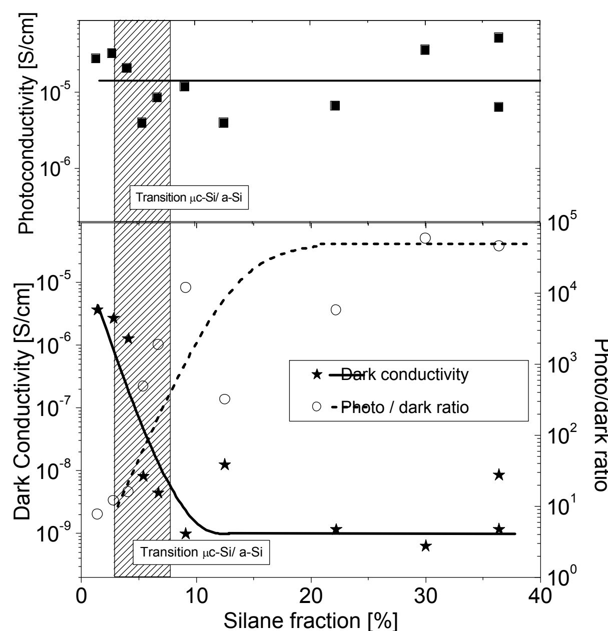

Figure 4. Dependence of photoconductivity, dark conductivity, and photo/dark ratio on the silane fraction.

The electrical properties of the layers are presented in Figure 4. The dark conductivity σ_{dark} shows a strong decrease with increasing silane fractions. This is the typical behavior that accompanies the transition from microcrystalline to amorphous structure. The photo conductivity σ_{ph} remains nearly constant (around 10^{-5} S/cm) in this range of silane fractions so that the ratio of $\sigma_{ph}/\sigma_{dark}$ follows approximately the inverse pattern of σ_{dark}. Thus, the transition can also be seen as a strong increase in $\sigma_{ph}/\sigma_{dark}$ with increasing silane fraction. The relatively high dark conductivity of the amorphous layers in the order of 10^{-10}-10^{-9} S/cm compared to values of 10^{-12} - 10^{-11} S/cm reported for device quality material [15], can at least partially be attributed to the lower band gap (E_{Tauc} = 1.5 – 1.6 eV compared to 1.7 – 1.8 eV for 'standard' layers) due to the higher deposition temperature of 300 °C of the layers presented here.

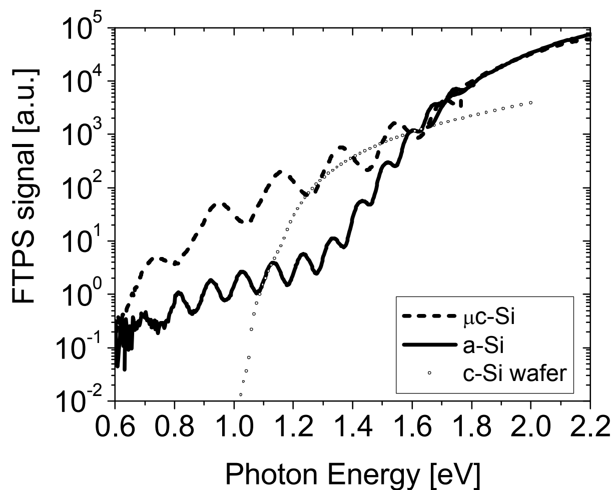

Figure 5. FTPS signal combined with UV-VIS absorption data for a microcrystalline Si layer deposited close to the transition region, and an amorphous layer.

The Urbach tail energy E_U, as derived from FTPS measurements in combination with absorption data obtained by UV-VIS spectroscopy (Fig. 5), is about 55 meV for the amorphous layers, and 107 meV for microcrystalline layers grown in the μc-Si/a-Si transition regime (silane fraction 5-8%). These values indicate a low defect density of the amorphous material, while for the microcrystalline layers further improvement is necessary.

4. Conclusions

A series of intrinsic amorphous and microcrystalline silicon films obtained with a variation of the silane flow in the source gas under otherwise constant deposition conditions has been deposited by Microwave PECVD. Compared to previous studies, a higher total pressure was used, and lower microwave power has been applied.

With increasing silane fraction, the silane utilization as well as the H_α/SiH^* ratio in the plasma decrease, and the layers become more amorphous. At the same time, the hydrogen content in the film and the refractive index of the material at 0.5 eV, an indicator for the density of the films, increase.

The best amorphous layers have a dark conductivity σ_{dark} of $6*10^{-10}$ S/cm, a photo/dark ratio $\sigma_{ph}/\sigma_{dark}$ of $6*10^4$, a microstructure factor R* below 0.1, and an Urbach tail Energy of 55 meV. For the microcrystalline layers close to the μc-Si/a-Si transition, a dark conductivity σ_{dark} of $1*10^{-6}$ S/cm, a photo/dark ratio $\sigma_{ph}/\sigma_{dark}$ of 16, and an Urbach tail Energy of 107 meV have been achieved.

This indicates that the higher pressure and lower microwave power during deposition compared to previous studies resulted in a strong improvement of the structural and opto-electrical properties of the microcrystalline and amorphous silicon layers deposited by microwave PECVD. Further optimization of deposition conditions is ongoing to improve the opto-electronical properties of the μc-Si layers. The next target will be to increase the deposition rate while maintaining the layer quality.

Acknowledgements

This work has been financially supported by the Dutch Ministry of Economic Affairs (Project No. TSIN3043) and the European Commission under contract no. INCO-CT-2004-509178.

References

[1] J. Meier, S. Dubail, R. Flückiger, D. Fischer, H. Keppner, and A. Shah, Proc. 1st World Conference and Exhibition on Photovoltaic Solar Energy Conversion, Hawaii,1994, pp 409-412.

[2] K. Yamamoto, A. Nakajima, M. Yoshimi, T. Sawada, S. Fukuda, T. Suezaki, M. Ichikawa, Y. Koi, M. Goto, T. Meguro, T. Matsuda, M. Kondo, T. Sasaki, Y. Tawada, Solar Energy, **77** (2004) 939.

[3] J. Meier, U. Kroll, E. Vallat-Sauvain, J. Spitznagel, U. Graf, and A. Shah, Solar Energy **77** (2004) 983.

[4] Y. Mai, S. Klein, R. Carius, J. Wolff, A. Lambertz, F. Finger, and X. Geng, J. Appl. Phys. **97** (2005) 114913.

[5] B. Rech, T. Roschek, T. Repmann, J. Müller, R. Schmitz, W. Appenzeller, Thin Solid Films **427** (2003) 157.

[6] R.E.I. Schropp, Thin Solid Films **451-452** (2004) 455-465.

[7] C. Smit, E.A.G. Hamers, B.A. Korevaar, R.A.C.M.M. van Swaaij, M.C.M. van de Sanden, J. Non-Cryst. Solids **299-302** (202) 98.

[8] W. Soppe, H. Rieffe, A. Weeber, Progr. in Photovolt. Res. Appl.., in press (2005).

[9] W.J. Soppe, A.C.W. Biebericher, C. Devilee, H. Donker, H. Schlemm, Proc. 3rd World Conference and Exhibition on Photovoltaic Solar Energy Conversion, Osaka, Japan, 2003.

[10] A.C.W. Biebericher, A.R. Burgers, C. Devilee, and W.J. Soppe, Proceedings 19th European Photovoltaic Solar Energy Conference, Paris, France (2004) 1485.

[11] W.J. Soppe, H.J. Muffler, A.C. Biebericher, C. Devilee, A.R. Burgers, A. Poruba, L. Hodakova, and M. Vanecek, Presented at the 20th European Photovoltaic Solar Energy Conference, Barcelona (2005).

[12] M.H. Brodsky, M. Cardona, and J.J. Cuomo, Phys. Rev. B **16** (1977), 3556.

[13] M. Vanecek and A. Poruba, Appl. Phys. Lett. **80** (2002) 719.

[14] P. Torres, U. Kroll, H. Keppner, J. Meier, E. Sauvain, and A. Shah, Proc. of the 5th European Conference on Thermal Plasma Processes, St. Petersburg, 1988, pp 855-860.

[15] R.E.I. Schropp, M. Zeman, *Amorphous and Microcrystalline Silicon Solar Cells - Modeling, Materials, and Device Technology*, Kluwer Academic Publishers, Norwell, Massachusets, USA, 1998.